STEM CELLS AND DEVELOPMENT
Volume 24, Number 6, 2015

DOI: 10.1089/scd.2014.0225

Label-Retaining Stromal Cells in Mouse Endometrium Awaken for Expansion and Repair After Parturition

Mingzhu Cao,[1,*] Rachel W.S. Chan,[1,2,*] and William S.B. Yeung[1,2]

Human and mouse endometrium undergo dramatic cellular reorganization during pregnancy and postpartum. Somatic stem cells maintain homeostasis of the tissue by providing a cell reservoir for regeneration. We hypothesized that endometrial cells with quiescent properties (stem/progenitor cells) were involved in the regeneration of the endometrial tissue. Given that stem cells divide infrequently, they can retain the DNA synthesis label [bromodeoxyuridine (BrdU)] after a prolonged chase period. In this study, prepubertal mice were pulsed with BrdU and after a 6-week chase a small population of label-retaining stromal cells (LRSC) was located primarily beneath the luminal epithelium, adjacent to blood vessels, and near the endometrial–myometrial junction. Marker analyses suggested that they were of mesenchymal origin expressing $CD44^+$, $CD90^+$, $CD140b^+$, $CD146^+$, and $Sca\text{-}1^+$. During pregnancy, nonproliferating LRSC predominately resided at the interimplantation/placental loci of the gestational endometrium. Immediately after parturition, a significant portion of the LRSC underwent proliferation ($BrdU^+/Ki\text{-}67^+$) and expressed total and active β-catenin. The β-catenin expression in the LRSC was transiently elevated at postpartum day (PPD) 1. The proliferation of LRSC resulted in a significant decline in the proportion of LRSC in the postpartum uterus. The LRSC returned to dormancy at PPD7, and the percentage of LRSC remained stable thereafter until 11 weeks. This study demonstrated that LRSC can respond efficiently to physiological stimuli upon initiation of uterine involution and return to its quiescent state after postpartum repair.

Introduction

The endometrium is hormone responsive and regenerates periodically during the reproductive lifespan [1]. Cyclic endometrium shedding, followed by proliferation and differentiation occurs in humans and other menstruating mammalians [1]. For mammals that do not menstruate like mice and rats, the endometrium undergoes cellular turnover of proliferation and apoptosis in each estrus cycle [2,3]. Other hallmarks of endometrial remodeling in both humans and mice are decidualization and postpartum involution [4]. For menstruating and nonmenstruating species, the stromal cells surrounding the implanting embryo undergo remarkable transformation in the early stages of pregnancy [5,6]. Signals generated by the decidual tissue and placenta are crucial to the maintenance of pregnancy and development of the fetuses [7,8]. Immediately after parturition, dynamic tissue repair processes, such as apoptosis, proliferation, extracellular matrix degradation, and reorganization, are involved in the remodeling of the endometrium [5,9–12]. The robust tissue destruction and remodeling during pregnancy and parturition in mice can be morphologically distinguished with the presence of discrete nodules along the side of the uterine horns. Each nodule represents a placentation site [13]. The uterus can increase more than 500-fold in volume and more than 20-fold in weight during pregnancy in humans [14]. After birth, separation of the placenta and the uterus results in a very thin endometrium. From day 7, postpartum regeneration of the endometrium begins. By day 26–56, the endometrium turns into an inactivated status and complete uterine involution [5]. To accomplish these extensive cellular turnover processes, the existence of somatic stem cells residing within the endometrium have long been proposed to play a role [15,16].

Somatic stem/progenitor cells can be quiescent or slow cycling when situated in their specific stem cell niche [17]. Somatic stem cells maintain tissue homeostasis by acting as a cell reservoir for tissue repair and regeneration [18,19]. A well-established technique for understanding the stem/progenitor cells and their microenvironment is the label-retaining cell (LRC) approach. LRCs are cells that retain a DNA synthesis label after a prolonged chase period. Rapidly dividing cells, such as transit-amplifying cells, dilute the label through cell divisions. An alternative explanation for LRCs is that a stem cell selectively transmits one DNA strand of each chromosome to a daughter stem cell, while the newly synthesized DNA strands are inherited by the other daughter

[1]Department of Obstetrics and Gynaecology and [2]Centre of Reproduction, Development of Growth, LKS Faculty of Medicine, University of Hong Kong, Pokfulam, Hong Kong, SAR, China.
*These two authors contributed equally to this work.

cells committed to differentiation, which will eventually be moved out of the tissue compartment [20,21]. The LRC approach has identified somatic stem/progenitor cells in various tissues, including the endometrium [15,22–24].

Proliferation of endometrial epithelial LRCs and some stromal LRCs from cycling mice can be induced by estrogen, consistent with their proposed role in endometrial regeneration [15]. A functional response of endometrial epithelial LRCs upon endometrial repair was also observed in an induced decidualization, breakdown, and repair mouse model [25,26]. Nonetheless, the role of endometrial LRCs in the remodeling processes during pregnancy and postpartum remains largely unknown. In this study, we sought to identify and study the temporal change in the proportion of LRCs in the gestational and postpartum mouse endometrium, an essential step toward understanding the involvement of putative stem cells in these remodeling events. Our findings revealed that a small population of endometrial stromal cells retained the bromodeoxyuridine (BrdU) label after a 6-week chase. Therefore, they were termed as label-retaining stromal cells (LRSC). These LRSC are in a quiescent state before and after extensive remodeling, but respond efficiently to stimuli upon initiation of uterine involution. The mobilization of LRSC is associated with activation of β-catenin.

Materials and Methods

Animal and housing condition

Mice were obtained from the Laboratory Animal Unit at The University of Hong Kong. All procedures conducted in this study were approved by the Committee on Use of Live Animals in Teaching and Research, The University of Hong Kong, Hong Kong. Mice were housed under standard laboratory conditions with a 12-h light/12-h dark cycle and free access to food and water.

Study design

The experimental setup is outlined in Figure 1A. Day 19 prepubertal C57BL/6J female mice were administered with BrdU intraperitoneally (50 μg/g of body weight; Sigma-Aldrich) twice daily for four consecutive days and allowed to grow without further labeling. After sexual maturity age, the mice were mated with >6-week-old fertile C57BL/6J male mice and pregnancy was confirmed by the presence of a vaginal plug. Three mice were sacrificed 4 h after the last BrdU injection (0-week chased) to determine the initial labeling index. Other mice were sacrificed at the following time points: 5-week chased (prepregnant, $n=3$), 5^+-week chased [gestational day; (GD)4, $n=3$], 6-week chased (GD7, $n=4$), 7-week chased (GD14, $n=3$), 8-week chased [postpartum day (PPD)1, $n=13$], 8^+-week chased (PPD3, $n=4$), 9-week chased (PPD7, $n=3$), 10-week chased (PPD14, $n=3$), and 11-week chased (PPD21, $n=4$,). Virgin age-matched mice were scarified at 5-week chased ($n=3$), 5^+-week ($n=3$), 6-week chased ($n=3$), 7-week chased ($n=3$), 8-week chased ($n=3$), 8^+-weeks ($n=3$), 9-week chased ($n=3$), 10-week chased ($n=3$), and 11-week chased ($n=3$) as controls. Mice were euthanized and the uterine horns were collected, fixed overnight with 4% paraformaldehyde, processed into paraffin blocks by standard technique, and analyzed for BrdU-labeled nuclei by immunohistochemistry and immunofluorescence (IF).

BrdU immunohistochemistry

Paraffin sections (5 μm) were dewaxed in xylene, rehydrated in descending alcohol series and finally in water, underwent antigen retrieval using an antigen retrieval buffer (Dako) in a microwave oven, denatured with 0.1 N HCl for 45 min at room temperature to allow the access of antibodies to single-stranded DNA, and quenched in 3% hydrogen peroxide/methanol for 10 min. Subsequently, the slides

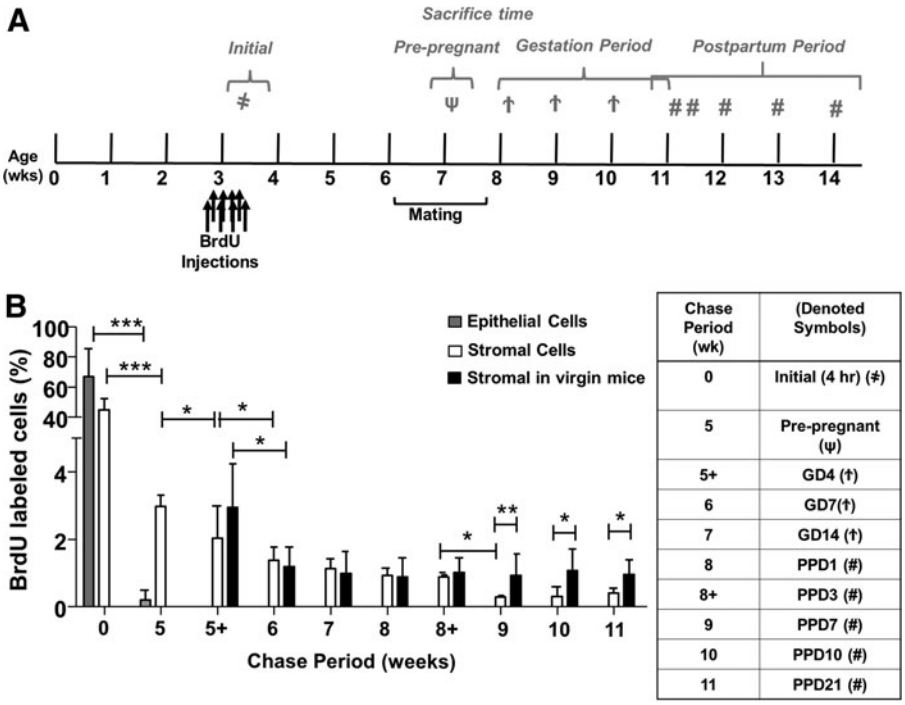

Chase Period (wk)	(Denoted Symbols)
0	Initial (4 hr) (≠)
5	Pre-pregnant (ψ)
5+	GD4 (†)
6	GD7(†)
7	GD14 (†)
8	PPD1 (#)
8+	PPD3 (#)
9	PPD7 (#)
10	PPD10 (#)
11	PPD21 (#)

FIG. 1. Quantitative analysis of BrdU-labeled cells in gestational and postpartum endometrium. **(A)** Timeline of the experimental methods. Prepubertal (day 19) C57BL/6J female mice were pulse labeled with BrdU (50 μg/g of body weight) twice daily for 4 days, and the label was then chased for up to 11 weeks. Female mice at 6 weeks of age were naturally mated with fertile males. Pregnant female mice were identified by vaginal plugs. Tissue was collected 4 h after initial labeling (as denoted by ≠), prepregnancy (as denoted by ψ), GD: 4, 7, 14 (as denoted by †), and PPD: 1, 3, 7, 14, 21 (as denoted by #). **(B)** BrdU-labeled cells are expressed as a percentage of total epithelial or stromal cells. Data are expressed as mean ± SEM, $n=3$–5 per group. BrdU, bromodeoxyuridine; GD, gestational days; PPD, postpartum days; SEM, standard error of the mean. $^*P<0.05$; $^{**}P<0.01$; $^{***}P<0.001$.

were blocked with 10% donkey serum (Sigma-Aldrich) in phosphate-buffered saline (PBS) for 1 h to reduce nonspecific binding, followed by successive incubation with sheep anti-BrdU antibody (1:800 dilution; Abcam) at 4°C overnight, polyclonal donkey anti-sheep biotinylated secondary antibodies (Abcam) for 1 h, and Vectastain ABC reagent (Vector Laboratories) for 30 min. The sections were examined under a Zeiss Axioskop II microscope (Carl Zeiss) for color development with the substrate 3, 3′-diaminobenzidine (Dako). Nuclei were counterstained with Mayer's hematoxylin for 30 s and washed with distilled water. The slides were mounted with the aqueous mounting medium (Dako) and images were captured using a Photometrics CoolSNAP digital camera (Roper Scientific). All incubations were performed at room temperature unless otherwise specified and washes with PBS were conducted between each step.

Dual IF staining

Paraffin sections were deparaffinized, rehydrated, antigen retrieved, denatured as described above, and blocked with 2% bovine serum albumin (BSA) in PBS for 30 min. For dual IF staining, the two primary antibodies were coincubated in 2% BSA at 4°C overnight in a humidified chamber. Secondary antibodies according to the host of the primary antibodies were diluted in 2% BSA and incubated for 1 h. For triple staining, anti-BrdU staining was performed first, followed by incubation of the appropriate primary antibodies at 4°C overnight and subsequently the corresponding secondary antibodies the next day. Nuclei were counterstained with 4,6-diamidino-2-phenylindole dihydrochloride (DAPI 1:1,000; Invitrogen Life Technologies) for 5 min and mounted with a fluorescence mounting medium (Dako). Multispectrum fluorescence images were acquired using a Carl Zeiss LSM 700 inverted confocal microscope and Zeiss LSM ZEN 2010 software (Carl Zeiss) at the University of Hong Kong Core Facility.

Antibodies

The dilution and details of the primary and secondary antibodies used for IF protocols are presented in Supplementary Tables S1 and S2 (Supplementary Data are available online at www.liebertpub.com/scd), respectively. Isotype-matched negative control immunoglobulin IgGs at the same concentration were included in each staining run. Tissue sections exposed to Alexa Fluor-conjugated secondary antibodies (488, 555 and 647) were also used as negative controls (Supplementary Fig. S1).

Enumeration of BrdU-labeled cells

For determination of $BrdU^+$ cells, the cells were counted in a blinded manner on one section of each transverse and longitudinal section from a single uterine horn from 3 to 5 mice per group for each time point. Images of the entire mouse uterus were captured by a digital camera (Roper Scientific). $BrdU^+$ cells and unstained ($BrdU^-$) cells in epithelial and stromal compartments were counted using ImageJ software (NIH Image; National Institutes of Health)—At least 10,000 nuclei per uterine horn per mouse at each time point. Only whole nuclei-stained BrdU cells were counted as labeled cells. Those that had the speckled BrdU appearance were not considered as LRSC. The percentage of $BrdU^+$ cells was determined by dividing the number of $BrdU^+$ cells by the total number of nuclei counted in each section.

Enumeration of cell surface marker and BrdU coexpressing cells

Double immunofluorescent-stained slides were viewed under the Carl Zeiss LSM 700 inverted confocal microscope, and the number of $BrdU^+Marker^+$ cells was counted using ImageJ software. The percentage of colocalizing cells was determined from two longitudinal and transverse sections from four BrdU-labeled mice at 12 weeks of chase. The percentage of $BrdU^+Marker^+$ cells was calculated by dividing the number of $BrdU^+Marker^+$ cells by the total number of nuclei counted in each section. The percentages are presented as mean ± standard error of the mean (SEM).

Statistical analysis

Data were analyzed using SPSS for Windows (version19.0; SPSS, Inc.). After testing for normal distribution using the D'Agostino-Pearson Kolmogorov-Smirnov test, statistical analysis was performed using Student's *t* test for comparisons of two independent groups. One-way analysis of variance followed by Fisher's least significant difference and Student–Newman–Keuls multiple comparisons post hoc tests were used for analysis of more than two independent groups. A difference with P-value < 0.05 is considered as significant. Data are represented as mean ± SEM.

Results

Gestational and postpartum endometrium contains label-retaining cells

To determine whether stem/progenitor cells were present during endometrial remodeling, we assessed the distribution of label-retaining cells in gestational and postpartum endometrium. Figure 1B shows the labeling index of BrdU in different chase periods. On day 0, after the labeling of prepubertal mice was completed, the BrdU labeling index was 66.8 ± 18.6% for epithelial and 44.5 ± 7.5% for stromal cells (Fig. 2A). Following a chase period of 5 weeks, only a few $BrdU^+$ epithelial cells were detected in the luminal epithelium (0.21 ± 0.28%, Fig. 2B) and were undetectable during gestation (Fig. 2C, D).

The percentage of $BrdU^+$ stromal cells also declined rapidly from 0- (∼45%) to 6-week chase (GD7: ∼1.4%, Fig. 2C, $P < 0.001$, Fig. 1B), but remained steady until parturition (Fig. 2D, E). Between PPD3 and PPD7, another significant decline of $BrdU^+$ cells occurred in the stromal compartment (PPD3: 0.88 ± 0.06%, Fig. 2F and PPD7: 0.28 ± 0.06%, Fig. 2G, $P < 0.05$, Fig. 1B). The percentage of $BrdU^+$ stromal cells was stable from the 9-week chase onward (PPD7, Fig. 2G and PPD14, Fig. 2H) and only a small proportion of labeled cells remained by the 11-week chase (PPD21: 0.41 ± 0.14%, Fig. 2I).

The percentage of LRSC decreases after parturition

To determine whether the endometrial stem/progenitor cells contributed to the remodeling events after pregnancy, we assessed the distribution of labeled-retaining cells in age-matched virgin mice. Following a chase period of 6 weeks, the

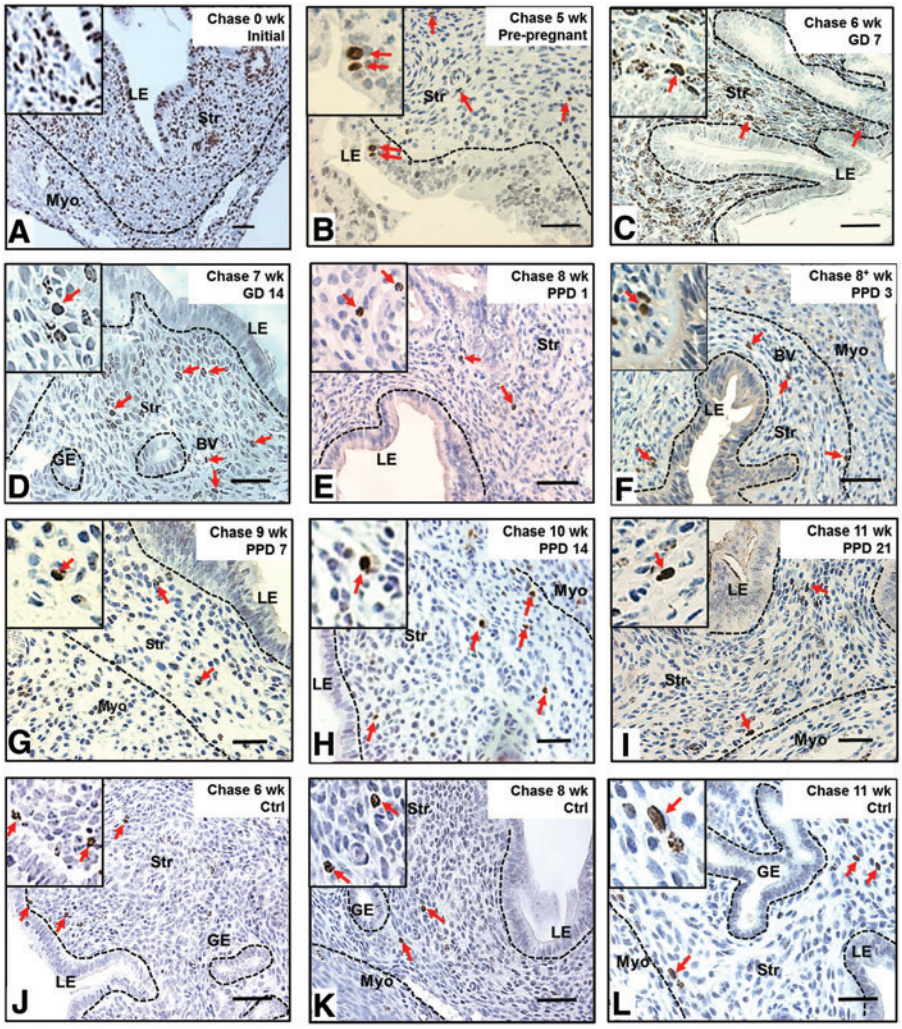

FIG. 2. Localization of label-retaining cells in **(A)** prepubertal, **(B)** prepregnant, **(C, D)** GD, **(E–I)** PPD, and **(J–L)** virgin mouse endometrium. **(A)** BrdU immunohistochemistry of prepubertal-labeled mouse uteri 4 h after the last injection (initial labeling, 0-week chase) showed majority of epithelial and stromal cells labeled with BrdU. **(B)** Before pregnancy, a few epithelial cells still retain BrdU labeling, but stromal BrdU-labeled cells rapidly declined. **(C, D)** During gestation, no epithelial BrdU-labeled cells were observed, and stromal BrdU-labeled cells were enriched in the nonimplantation/placental locus. **(E–I)** From PPD3 to PPD21, several LRSC localized in the vicinity of blood vessels and adjacent to the luminal epithelium or endometrial–myometrium junction. **(J–L)** Stromal BrdU-labeled cells were detected in virgin mice at similar locations as remodeling mice. *Inserts* are enlarged figures of BrdU-labeled cells at different time points. *Red arrows* show the distribution of BrdU-labeled cells. LE, luminal epithelium; GE, glandular epithelium; Str, stroma; Myo, myometrium; BV, blood vessel; LRSC, label-retaining stromal cells. Scale bar: 5 μm. Color images available online at www.liebertpub.com/scd

normal cycling endometrium in virgin mice contained a small percentage of BrdU-labeled stromal cells (1.19 ± 0.58%) and remained unchanged at the 11-week chase (0.96 ± 0.43%, Figs. 1B and 2J–L). A similar percentage of $BrdU^+$ stromal cells was found in the gestational endometrium of the same chased period (GD7: 1.36 ± 0.39%; $P = 0.763$). We termed these stromal cells after a 6-week chase as LRSC. For virgin females, or those who had undergone gestation/postpartum remodeling, the locations of LRSC were found in the following three regions: beneath the luminal epithelium (Fig. 2F, H, J), adjacent to blood vessels (Fig. 2E, I), and near the endometrial–myometrial junction (Fig. 2H, I, L). Interestingly, we noticed that the LRSC at the 11-week chase were significantly higher in age-matched virgins compared with mice that had undergone gestation and postpartum remodeling (0.96 ± 0.43% vs. 0.41 ± 0.14%, respectively, $P < 0.05$, Fig. 1B).

Surface phenotype of LRSC

Given that mouse endometrial stem/progenitor cells had no known cell surface markers, we evaluated their expression with a series of different surface markers (Table 1). Double IF of LRSC at PPD21 demonstrated that these cells express CD140b (Fig. 3A), CD146 (Fig. 3B), CD44 (Fig. 3C), CD90 (Fig. 3D), Sall4 (Fig. 3E), and Sca-1 (Fig. 3F), and are negative for ABCG2 (Supplementary Fig. S2A) and Musashi-1 (Supplementary Fig. S2B). There were wide variations in the expression pattern of these markers, ranging from 1.8% to 72% of the LRSC population (Table 1; Fig. 3G and Supplementary Fig. S3).

LRSC reside in the interimplantation loci of the endometrium during gestation

The gestational endometrium is characterized by distinct implantation sites (Fig. 4A). Given that connexin 43 is a widely

TABLE 1. EXPRESSION OF SURFACE MARKERS ON LABEL-RETAINING STROMAL CELLS

Markers	*Expression on LRSC (%)*
CD140b	44.51 ± 2.33
CD146	1.81 ± 0.37
CD44	23.72 ± 2.25
CD90	45.26 ± 12.88
Sall4	33.97 ± 0.90
Sca1	72.03 ± 15.01
ABCG2	0
Musashi-1	0

LRSC, label-retaining stromal cells.

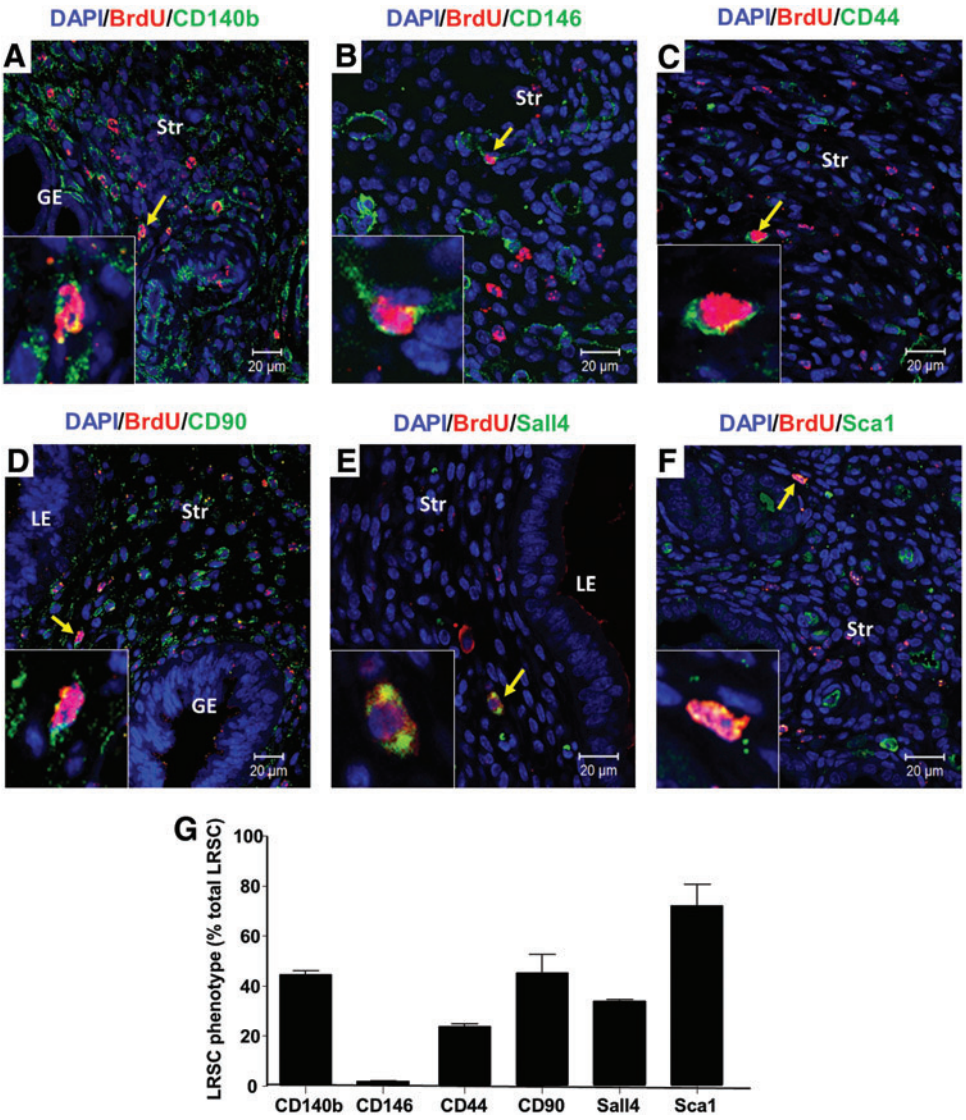

FIG. 3. Phenotypic characterization of LRSC with various surface markers. Immunofluorescence images showing the LRSC and their colocalization (*yellow arrow*) with **(A)** CD140b, **(B)** CD146, **(C)** CD44, **(D)** CD90, **(E)** Sall4, and **(F)** Sca-1 at PPD21. *Inserts* are enlarged figures of LRSC coexpressing different phenotypic markers. **(G)** The percentage of LRSC coexpressing various surface markers. Data are expressed as mean ± SEM, $n = 3$ per group. Scale bar: 20 μm. Color images available online at www.liebertpub.com/scd

used implantation marker in murine models and localized distinctively in implantation/placental loci [27–30], this marker was used to assess the spatial distribution of LRSC during gestation (GD7, 14) and the early postpartum (PPD1) period. The connexin 43 expression was restricted to the implantation/placental loci of the gestational endometrium (Fig. 4C[ii]) and commonly associated with distinct large decidualized cells depicted by their round nucleus (Fig. 4D[i], [ii]).

Figure 4B revealed that the LRSC were prominently enriched in interimplantation/placental loci of the GD7 (Fig. 4D[i]), GD14 (Fig. 4D[iii]), and PPD1 endometrium (Fig. 4D[v]). Significantly more LRSC resided within the interimplantation/placental loci (Fig. 4D[i], [iii], [v]) compared with the implantation/placental (Fig. 4D[ii], [iv], [vi]) loci (GD7: 18.31 ± 2.04% vs. 0.84 + 0.16%, $P < 0.01$; GD14: 12.43 ± 0.65% vs. 0%, $P < 0.05$; PPD1: 3.23 ± 0.45% vs. 0.54 ± 0.23%, $P > 0.05$, Fig. 4B). Although LRSC were exclusively located in the interimplantation/placental loci of the endometrium at GD14, these cells soon distributed throughout the endometrium by PPD1 (Fig. 4[v], [vi]) and PPD3 after parturition (data not shown).

LRSC proliferate upon parturition

We assessed the ability of LRSC to proliferate in response to stimuli during gestation and postpartum. Figure 5A shows the distribution of proliferating LRSC ($Ki67^+/BrdU^+$) in the gestational (GD14) and postpartum endometrium (PPD1, 3). At the midgestational period (GD7 and 14) no proliferating LRSC were detected, suggesting that they were quiescent during this period (Fig. 5A[i], B). Dual IF revealed that the colocalization of Ki67 with BrdU was restricted to the endometrium at PPD1 (Fig. 5A[ii]) and PPD3 (Fig. 5A[iii]). The highest percentage of proliferating LRSC occurred at PPD1 (43.89 ± 5.36%) and declined significantly at PPD3 (18.20 ± 0.83%, $P < 0.05$, Fig. 5A). Thus, LRSC were immediately active after parturition and their proliferative ability declined thereafter. Aside from proliferating LRSC, some nonproliferating LRSC persisted ($Ki67^-/BrdU^+$, Fig. 5A[ii], [iii]) during postpartum. Since proliferating LRSC were detected at PPD1 and PPD3, this resulted in the lower proportion of LRSC detected at PPD7 (PPD3: 0.88 ± 0.06% vs. PPD7: 0.28 ± 0.06%, $P < 0.05$,

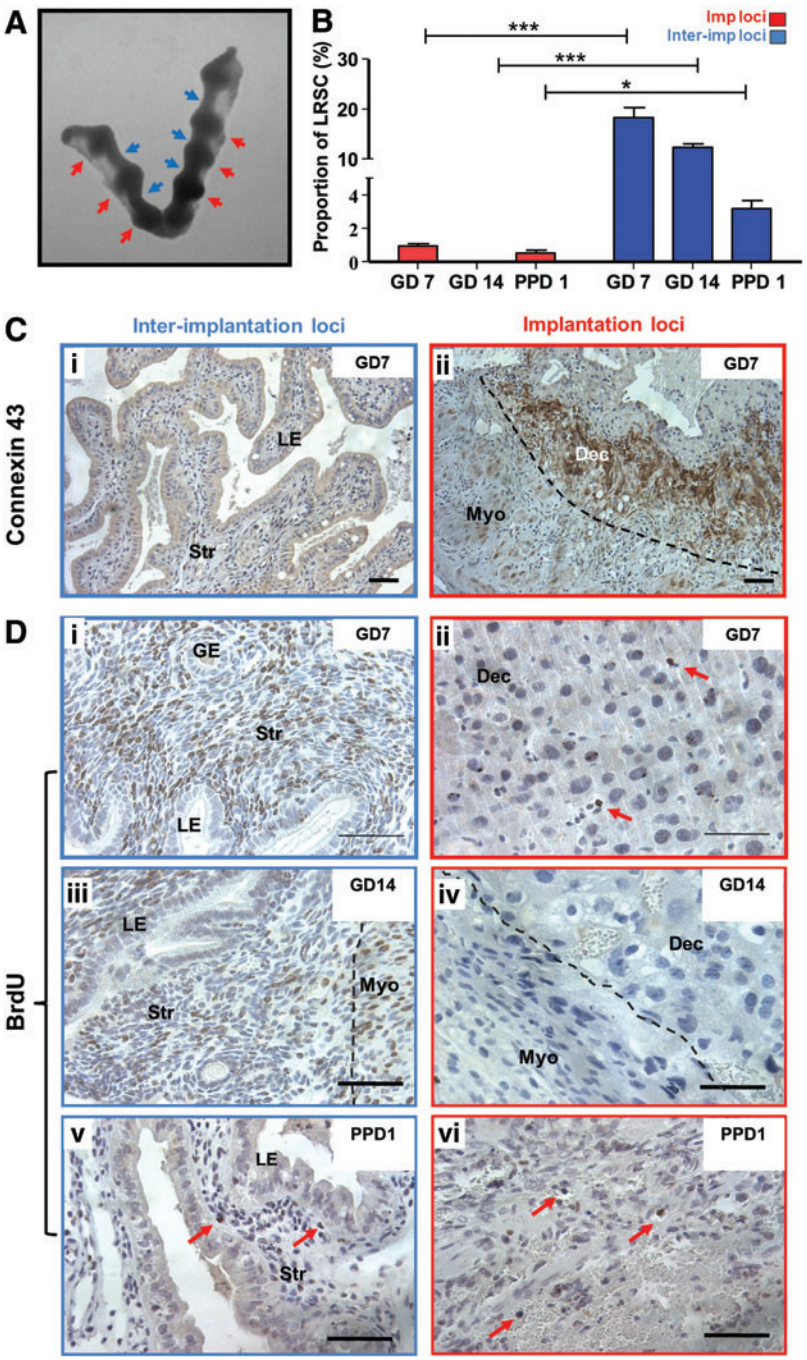

FIG. 4. Spatial distribution of LRSC within the pregnant and early postpartum endometrium. **(A)** Mouse uterine horns at GD7 showing the implantation/placental loci (*red arrowheads*) and interimplantation/placental loci (*blue arrowheads*). **(B)** The percentage of LRSC in interimplantation/placental loci and implantation/placental loci at different gestational and postpartum time points. **(C)** Immunohistochemical staining of connexin 43 (*brown*) localizing in the **(ii)** implantation/placental loci of GD7 endometrium compared with the **(i)** interimplantation/placental loci. **(D)** Representative BrdU immunohistochemistry staining (*brown, red arrows*) showing LRSC enriched in interimplantation/placental loci (*left panel*) of **(i)** GD7, **(iii)** 14, and **(v)** PPD1 mouse uterus. Fewer LRSC were found within implantation/placental loci (*right panel*) of **(ii)** GD7, **(iv)** 14, and **(vi)** PPD1 mouse endometrium. Data are expressed as mean ± SEM, $n = 3$ per group. Dec, decidua; Imp loci, implantation/placental loci; InterImp loci, interimplantation/placental loci. $*P < 0.05$, $***P < 0.001$. Scale bar: 5 μm. Color images available online at www.liebertpub.com/scd

Fig. 1B) and a higher amount of LRSC present in virgin mice at the 11-week chase (PPD21: 0.96 ± 0.43% vs. virgin: 0.41 ± 0.14%, $P < 0.05$, Fig. 1B).

Activated LRSC expressed the Wnt/β-catenin signal pathway components

The Wnt/β-catenin signaling pathway plays an important role in stem cell self-renewal in vivo and in vitro [31,32], asymmetric cell division of stem cells [33], and is a key mediator of human endometrial homeostasis and proliferation [34]. Therefore, we investigated the expression of total β-catenin and its active form in LRSC. The expression of total β-catenin (Fig. 6A) and active β-catenin (ABC) (Fig. 6B) on LRSC at PPD1 was 34.50 ± 13.17% and 7.95 ± 4.64%, respectively (Fig. 6C). In virgin mice, 14.17 ± 11.76% of LRSC expressed total β-catenin and no LRSC expressed ABC (Fig. 6C). Moreover, higher proportions of LRSC at PPD1 coexpressed with total β-catenin and ABC than other gestational and PPDs (Fig. 6D, E). Notably, 9.95 ± 1.89% of LRSC coexpressed with Ki67 and total β-catenin (Fig. 6F, G[i]), and 5.27 ± 0.91% of LRSC coexpressed with Ki67 and ABC at PPD1 (Fig. 6F, G[ii]). The coexpression of Ki67 with total β-catenin or ABC was not detected in virgin mice (Fig. 6F).

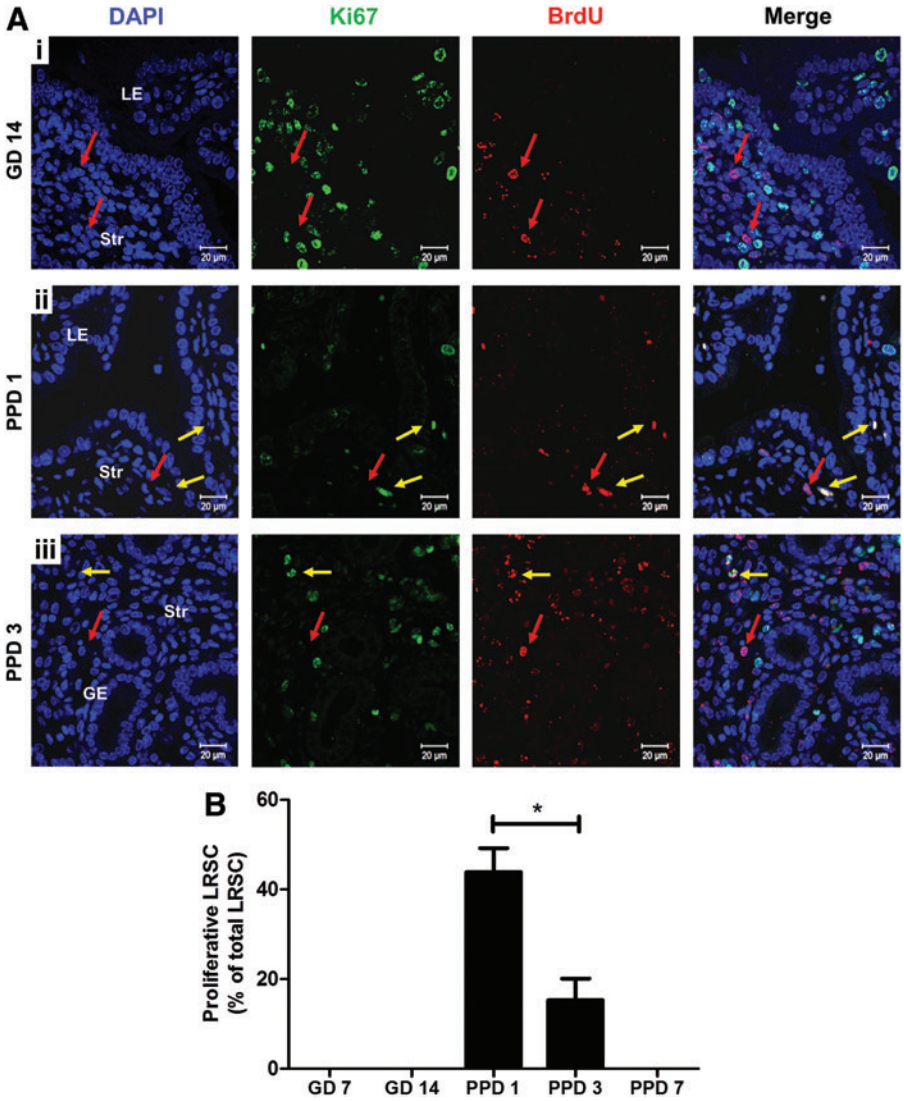

FIG. 5. Proliferation of LRSC. **(A)** Representative immunofluorescent images showing LRSC colocalizing with proliferating marker Ki67 (*yellow arrow*) at **(ii)** PPD1 and **(iii)** PPD3. No colocalization with Ki67 (*red arrow*) for LRSC at GD7 and **(i)** GD14 uterus. **(B)** The percentage of proliferating LRSC at different gestational and postpartum time points. Data are expressed as mean ± SEM, $n = 3–5$ per group. $^*P < 0.05$. Scale bar: 20 μm. Color images available online at www.liebertpub.com/scd

Identification of endometrium epithelial BrdU$^+$ cells after parturition

The high cellular turnover of epithelial cells at gestation resulted in depletion of epithelial BrdU$^+$ cells from the 5$^+$-week chase (GD4, Fig. 1B). Interestingly, at PPD1, a few epithelial cells with strong nuclei BrdU staining were observed in the luminal epithelium (Fig. 7A, B) and none in the glandular epithelium. The time of tissue collection after parturition was a crucial factor for the identification of these epithelial BrdU$^+$ cells. Of the 10 mice analyzed at PPD1, only two mice harvested within 6 h after parturition contained occasional epithelial BrdU$^+$ cells.

The reappearance of epithelial BrdU cells in the luminal epithelium, led to the investigation of surrounding LRSC at PPD1. We found postpartum females containing a higher proportion of LRSC beneath the luminal epithelium (within one-cell diameter) compared with age-matched virgin mice (26.13 ± 9.08% vs. 8.20 ± 4.36%, $P < 0.05$, Fig. 7B–D).

Discussion

Adult stem cells are rare specialized cells that self-renew and differentiate to supply a progeny of lineage-specific cells for cellular replacement after injury-like events [35]. Despite the identification of stem cells in endometrial homeostasis, the roles of these cells in highly dynamic states such as pregnancy and postpartum remain unclear. Using the BrdU pulse-chase experiment, this study investigated the in vivo location of LRSC and their possible role in uterine regeneration. If all endometrial cells divide evenly during uterine remodeling, this would cause homogenous dilution and eventual loss of the label, like the pancreas [36]. Instead, the identification of cells retaining BrdU label after an 11-week chase in the virgin females indicates some endometrial cells divide much less frequently than the surrounding cells or may have undergone asymmetric division. In addition, we demonstrate the functional activity of LRSC in response to parturition stimuli.

LRSC in the gestational and postpartum endometrium

The mouse endometrium is a highly renewing adult tissue in mammals and serves as an excellent model for studying the role of tissue stem/progenitor cells in response to local

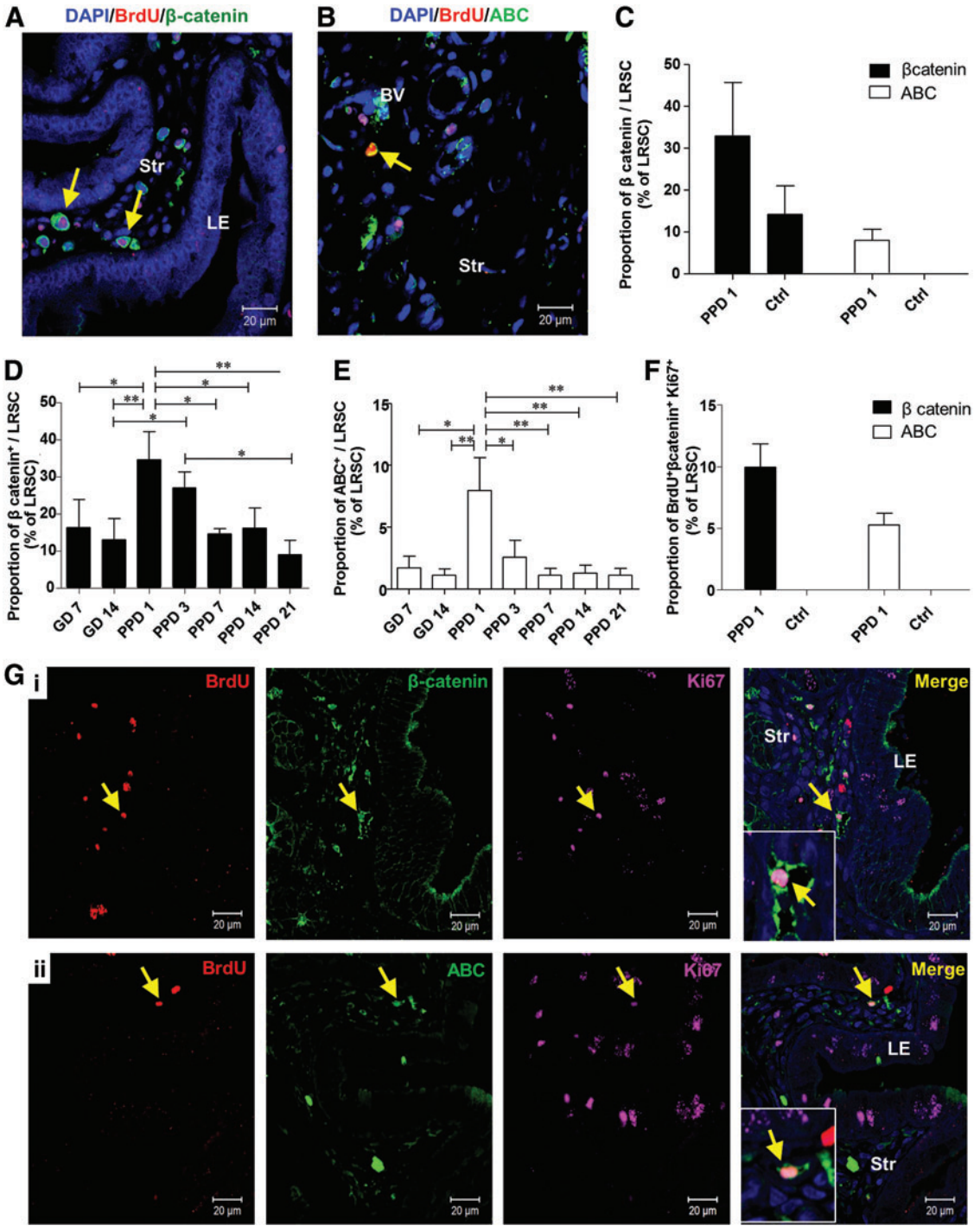

FIG. 6. Proliferating LRSC express total β-catenin and ABC. Representative immunofluorescence images show LRSC at PPD1 colocalizing with **(A)** β-catenin (*yellow arrow*) and **(B)** ABC (*yellow arrow*). **(C)** The percentage of LRSC coexpressing β-catenin and ABC in PPD1 and virgin mice. The percentage of LRSC coexpressing β-catenin **(D)** and ABC **(E)** at different gestational and postpartum time points. **(F)** The colocalization of LRSC with both β-catenin/Ki67 and ABC/Ki67 in PPD1 and virgin mice. **(G)** Representative figures show the triple staining of either **(i)** BrdU/β-catenin/Ki67 (*yellow arrow*) or **(ii)** BrdU/ABC/Ki67 (*yellow arrow*). *Inserts* are enlarged figures of LRSC coexpressing two proteins. Data are expressed as mean ± SEM, $n = 3$–5 per group. ABC, active β-catenin; Ctrl, virgin mice. $^{*}P < 0.05$, $^{**}P < 0.01$. Scale bar: 20 μm. Color images available online at www.liebertpub.com/scd

niche stimuli. In an artificial mouse endometrial repair model, LRSC near vasculatures proliferate upon tissue breakdown [25]. On the other hand, LRCs enriched at the distal oviduct and the endocervical transition zone did not respond to endometrial regeneration events [37]. These findings support the existence of a functional stem cell compartment in the mouse endometrium. Since, decidualization and postpartum involution are hallmarks of endometrial remodeling events [4], we examined the location of the LRSC during pregnancy and at postpartum.

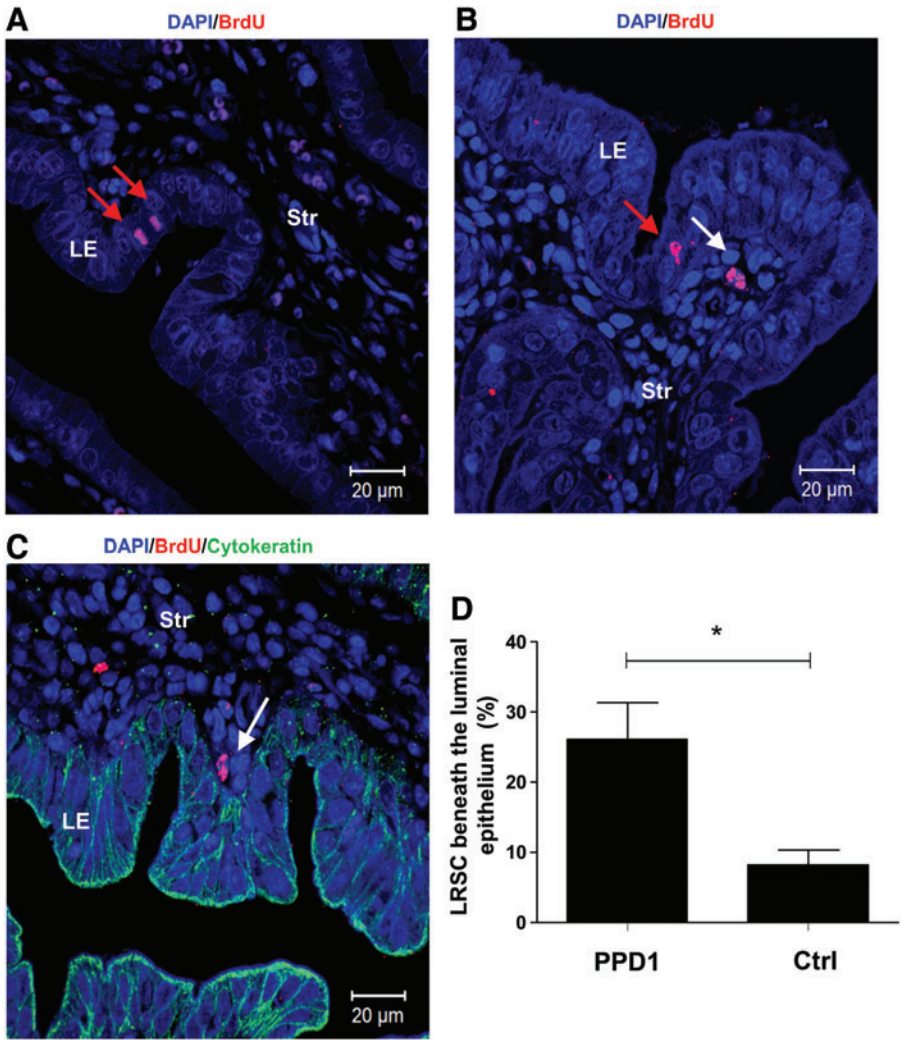

FIG. 7. Identification of epithelial BrdU$^+$ cells and location of LRSC on PPD1. **(A)** Epithelial BrdU$^+$ cells in the luminal epithelium (*red arrow*) and **(B)** LRSC (*white arrow*) were detected within 6 h after parturition. **(C)** PPD1 endometrium was double immunostained with BrdU (*red*) and cytokeratin (*green*) to visualize LRSC in proximity to the luminal epithelium (*white arrow*). **(D)** Percentage of LRSC beneath the luminal epithelium (within one-cell diameter). Data are expressed as mean ± SEM, $n = 3$ per group. *$P < 0.05$. Scale bar: 20 μm. Color images available online at www.liebertpub.com/scd

As expected, the extensive structural and functional differentiation during early pregnancy resulted in a significant decline of LRSC. In this study, the percentage of BrdU$^+$ cells in the virgin mice and the pregnant mice dropped within the duration of the chase period and reached the same stable level after a 6-week chase. We termed these cells LRSC, and they could represent the endometrial stromal stem/progenitor cell population.

Although the LRC approach has been widely used to study the distribution and functions of putative stem cells in different adult tissues, it is not specific for stem cells. Arrest cells in vivo may also retain the BrdU label, hence producing false-positive errors. Since our LRSC were able to proliferate upon specific stimuli, it is unlikely that such a phenomenon occurred in this study.

The histological and morphological appearance of the uterine horns returned to its nonpregnant state in less than 1 week after parturition. Hence, after completion of endometrial remodeling only 0.4% of LRSC remained at PPD21 and resided in regions reported in cycling mice, that is, beneath the luminal epithelium, around the blood vessels, and near the myometrium–endometrium junction [15].

The phenotypic characterization of LRSC

Several evidences suggest that endometrial repair can trigger recruitment of endometrial stem/progenitor cells from the bone marrow through vasculature [25,38]. Hence, we examined three markers (CD44, CD90, and Sca-1), which have been reported to be expressed on mesenchymal stem-like cells in the female reproductive system, including the human endometrium [39], myometrium [14], menstrual blood [40], and mammary glands [41]. The percentage of LRSC expressing CD44$^+$ and CD90$^+$ were 23.72 ± 2.25% and 45.26 ± 12.88%, respectively, suggesting that a significant proportion of the endometrial stem/progenitor cells could be of mesenchymal origin. Interestingly, 72.04 ± 15.01% of the LRSC were Sca-1$^+$, a marker used to enrich hematopoietic stem cells, mammary stem/progenitor cell, and other mesenchymal stem cells [42]. Previous work demonstrated that LRSC in the cycling endometrium, myometrium, and distal oviduct lack Sca-1 expression [43,44]. However, endometrial postpartum cells with a side population phenotype showed abundant expression of Sca-1 [45]. The discrepancies in these observations may be related to difference in the studied cell populations (eg, LRSC vs. side

population) and/or physiological state of the animals (eg, estrus cycling vs. postpartum). In general, decidualized endometrial stromal cells express abundant amount of Sca-1 during implantation [46].

In the human endometrium, stromal cells coexpressing perivascular markers, CD146 and CD140b, exhibit stem cell-like activity based on in vitro assays and differentiation ability [47]. About half of the LRSC expressed CD140b ($44.51 \pm 2.33\%$), but the CD146 expression was very low ($1.81 \pm 0.37\%$). Hence, we speculate that the putative stem/progenitor cell population in mice may not share the same phenotype as in humans [47]. This aside, we also evaluated several cellular markers related to stem cells, but were unable to identify a marker signature that uniquely identifies LRSC in the mouse endometrium. Thus, there is still no specific marker for mouse endometrial stem/progenitor cells.

Environmental niches and LRSC

During pregnancy. Depending on the environmental cues, niche cells can maintain stem cells in an undifferentiated state or mobilize resident stem cells to function [48,49]. During pregnancy, nonproliferating LRSC preferentially localize within the interimplantation sites during the late gestational stage, suggesting that these regions maintain the LRSC in a quiescent state. The lack of cell proliferation regulator genes (cyclin D1, D2, and D3) in the interimplantation sites in comparison with the implantation sites [50] supports that these sites are relatively dormant. Such a microenvironment would be critical for maintaining a reservoir of LRSC after each successive pregnancy.

Postpartum remodeling. The regeneration of the endometrium occurs immediately after parturition [51,52]. Therefore, it was not surprising that a proportion of the LRSC proliferated soon after parturition (PPD1). We speculate that the LRSC are activated to reorganize the endometrium after the birth of newborns. The distinct proliferating LRSC subset identified after parity may correspond to the repopulating cells. A similar observation occurs in the mammary compartments [53]. To protect stem cell exhaustion, these cells exhibit increased cell proliferation and differentiation, but are able to return to dormancy through inhibitory signals from the niche environment. Such a functional response of the stem cells to physiological and pathological stimulations is a common phenomenon in a variety of tissues, including the skin [48,54,55], intestine [49,55,56], mammary gland [41], and pancreas [57]. These adult stem cells must be mobilized periodically to generate cells committed to replenish certain cell lineages [58]. Bulge LRCs expelled from their niche, migrate upward [55], and proliferate to repair the damaged skin epidermis [59]. Hematopoietic stem cells respond readily to injuries and reversibly switch to dormancy after reestablishment of homeostasis [60]. In the rat kidney, papillary LRCs migrate toward other regions of the kidney, and proliferate after acute kidney injury [22]. In the mouse ovary, H2B-GFP LRCs are quiescent before ovulation and proliferate upon estrous cycling changes [23]. In this study, we demonstrate that certain LRSC at the interimplantation/placental loci during pregnancy can facilitate the endometrial remodeling after parturition.

Wnt/β-catenin signaling pathway involvement in the activation of LRSC

The role of the Wnt/β-catenin signaling pathway on stem cell function is well documented. Habib et al. [33] demonstrated that Wnt directed the mitotic division plane and oriented the asymmetric distribution of the centrosome in embryonic stem cells. Lowry et al. showed β-catenin acted directly on the stem cells of the hair follicle to induce their mobilization or exit from a quiescent state to provide proliferating transit-amplifying cells [61]. In mouse mammary stem cells, the Wnt protein can promote their long-term expansion [62].

In this study, we found greater expression of total β-catenin and active β-catenin in LRSC at PPD1 compared with the virgin age-matched mice. Such a phenomenon was only detected after partition and not in other gestation and postpartum periods. This finding provides the first evidence on the possible role of the Wnt/β-catenin signaling pathway on the activation of putative stem/progenitor cells in the mouse endometrial regeneration. Further investigation is necessary to understand the mechanisms of the Wnt/β-catenin pathway on endometrial stem/progenitor cell activation.

LRSC may facilitate the regeneration of the epithelium during the postpartum period

After parturition and expulsion of the placenta, the epithelial basement membrane is completely lost in the first 24 h. An incomplete layer of epithelial cells and stroma containing numerous microvasculatures reappears by 48 h. These observations reflect that the regeneration takes place immediately and rapidly after parturition. In this study, no epithelial $BrdU^+$ cells were observed during pregnancy. At PPD1, a few epithelial $BrdU^+$ cells reappeared in the luminal epithelium. The number of LRSC beneath the luminal epithelium in these mice was significantly more compared with the virgin mice. Previously, using genetic fate-mapping techniques, Huang et al. proved that a proportion of stromal cells differentiates into both luminal and glandular epithelial cells after parturition and contributes to the reepithelialization process [63]. Our observations, together with other reports, provide evidences that the endometrial epithelial cells in mice could be derived from the stromal cells during endometrial regeneration [63,64].

We speculate that the transformation of LRSC into epithelial cells requires mesenchymal–epithelial transition (MET). Patterson et al. [64] demonstrated MET in epithelial repair after decidualization. Notably, cells in the transitional state between the mesenchyme ($vimentin^+$) and epithelium ($pan\text{-}cytokeratin^+$) were found migrating from the endometrium–myometrium junction to the lumen to facilitate the reepithelialization after artificial decidualization. During MET, the mesenchymal cells progressively lose their mesenchymal traits and obtain the epithelial characteristics [65]. In this study, LRSC located near the luminal epithelium did not express cytokeratin, suggesting that these cells are in the initial stages of the MET.

Since, there were abundantly more LRSC locating near the luminal epithelium in the PPD1 endometrium than in virgin mice, we propose that LRSC may have the ability to migrate to the disrupted luminal epithelium and transform

into epithelial-like cells for reepithelialization after parturition, suggestive of a dual epithelial/stromal differentiation potential. Interestingly, similar cyclic rupture, repair, and regeneration occur in the ovary after each ovulation. Resident stem cells located in the coelomic epithelium at the sites of the ovulation wound can facilitate repeated reepithelialization processes and display characteristics of epithelia and mesenchyme [23]. These data strengthen our theory that in preparation for the remodeling of the endometrium after giving birth, certain environment cues may elicit surrounding LRSC to proliferate and undergo MET for the reconstitution of the epithelial compartment in postpartum endometrium. However, we cannot exclude the possibility that the epithelial $BrdU^+$ cells may originate from a circulating source such as the bone marrow. Morelli et al. [66] showed bone marrow cells can serve as a cellular source for cyclic replenishment of multiple endometrial cell types. Bone marrow-derived stem cells can transdifferentiate into endometrial epithelial and stromal cells [67]. They also contribute toward the regeneration of the endometrium after ischemia/reperfusion injury [68].

In conclusion, we identified and characterized mouse endometrial LRSC after dramatic physiological remodeling. LRSC primarily located in the interimplantation loci proliferated after parturition and highlight the possible involvement of the Wnt/β-catenin pathway in endometrial stem cell activation. It is essential that future studies examine the role of the Wnt/β-catenin pathway on endometrial stem cell regulation.

Acknowledgments

The authors thank all the staff at the Laboratory Animal Unit and Faculty Core Facility, the University of Hong Kong, for their assistance in this study. This work was supported by a grant from the General Research Fund (GRF), Research Grant Council (HKU 7822/09M) to W.S.B.Y.

Author Disclosure Statement

The authors declare no financial or commercial conflicts of interest.

References

1. Gargett CE and H Masuda. (2010). Adult stem cells in the endometrium. Mol Hum Reprod 16:818–834.
2. Wood GA, JE Fata, KL Watson and R Khokha. (2007). Circulating hormones and estrous stage predict cellular and stromal remodeling in murine uterus. Reproduction 133: 1035–1044.
3. Gargett CE, RW Chan and KE Schwab. (2007). Endometrial stem cells. Curr Opin Obstet Gynecol 19:377–383.
4. Ramathal CY, IC Bagchi, RN Taylor and MK Bagchi. (2010). Endometrial decidualization: of mice and men. Semin Reprod Med 28:17–26.
5. Salamonsen LA. (2003). Tissue injury and repair in the female human reproductive tract. Reproduction 125:301–311.
6. Fazleabas AT and Z Strakova. (2002). Endometrial function: cell specific changes in the uterine environment. Mol Cell Endocrinol 186:143–147.
7. Candeloro L and TM Zorn. (2007). Granulated and nongranulated decidual prolactin-related protein-positive decidual cells in the pregnant mouse endometrium. Am J Reprod Immunol 57:122–132.
8. Parr MB, HN Tung and EL Parr. (1986). The ultrastructure of the rat primary decidual zone. Am J Anat 176:423–436.
9. Bae HS, KH Ahn, MJ Oh, HJ Kim and SC Hong. (2012). Postpartum uterine involution: sonographic changes in the endometrium between 2 and 6 weeks postpartum related to delivery mode and gestational age at delivery. Ultrasound Obstet Gynecol 39:727–728.
10. Takamoto N, PC Leppert and SY Yu. (1998). Cell death and proliferation and its relation to collagen degradation in uterine involution of rat. Connect Tissue Res 37:163–175.
11. Alan E and N Liman. (2012). Immunohistochemical localization of beta defensins in the endometrium of rat uterus during the postpartum involution period. Vet Res Commun 36:173–185.
12. Balbin M, A Fueyo, V Knauper, AM Pendas, JM Lopez, MG Jimenez, G Murphy and C Lopez-Otin. (1998). Collagenase 2 (MMP-8) expression in murine tissue-remodeling processes. Analysis of its potential role in postpartum involution of the uterus. J Biol Chem 273:23959–23968.
13. Brandon JM. (1990). Decidualization in the post-partum uterus of the mouse. J Reprod Fertil 88:151–158.
14. Ono M, T Maruyama, H Masuda, T Kajitani, T Nagashima, T Arase, M Ito, K Ohta, H Uchida, et al. (2007). Side population in human uterine myometrium displays phenotypic and functional characteristics of myometrial stem cells. Proc Natl Acad Sci U S A 104:18700–18705.
15. Chan RW and CE Gargett. (2006). Identification of label-retaining cells in mouse endometrium. Stem Cells 24:1529–1538.
16. Padykula HA. (1991). Regeneration in the primate uterus: the role of stem cells. Ann N Y Acad Sci 622:47–56.
17. Barker N, S Bartfeld and H Clevers. (2010). Tissue-resident adult stem cell populations of rapidly self-renewing organs. Cell Stem Cell 7:656–670.
18. Mothe AJ and CH Tator. (2005). Proliferation, migration, and differentiation of endogenous ependymal region stem/progenitor cells following minimal spinal cord injury in the adult rat. Neuroscience 131:177–187.
19. Beltrami AP, L Barlucchi, D Torella, M Baker, F Limana, S Chimenti, H Kasahara, M Rota, E Musso, et al. (2003). Adult cardiac stem cells are multipotent and support myocardial regeneration. Cell 114:763–776.
20. Cairns J. (1975). Mutation selection and the natural history of cancer. Nature 255:197–200.
21. Escobar M, P Nicolas, F Sangar, S Laurent-Chabalier, P Clair, D Joubert, P Jay and C Legraverend. (2011). Intestinal epithelial stem cells do not protect their genome by asymmetric chromosome segregation. Nat Commun 2:258.
22. Oliver JA, A Klinakis, FH Cheema, J Friedlander, RV Sampogna, TP Martens, C Liu, A Efstratiadis and Q Al-Awqati. (2009). Proliferation and migration of label-retaining cells of the kidney papilla. J Am Soc Nephrol 20:2315–2327.
23. Szotek PP, HL Chang, K Brennand, A Fujino, R Pieretti-Vanmarcke, C Lo Celso, D Dombkowski, F Preffer, KS Cohen, J Teixeira and PK Donahoe. (2008). Normal ovarian surface epithelial label-retaining cells exhibit stem/progenitor cell characteristics. Proc Natl Acad Sci U S A 105:12469–12473.
24. Karpowicz P, C Morshead, A Kam, E Jervis, J Ramunas, V Cheng and D van der Kooy. (2005). Support for the immortal

strand hypothesis: neural stem cells partition DNA asymmetrically in vitro. J Cell Biol 170:721–732.
25. Kaitu'u-Lino TJ, L Ye, LA Salamonsen, JE Girling and CE Gargett. (2012). Identification of label-retaining perivascular cells in a mouse model of endometrial decidualization, breakdown, and repair. Biol Reprod 86:184.
26. Kaitu'u-Lino TJ, L Ye and CE Gargett. (2010). Re-epithelialization of the uterine surface arises from endometrial glands: evidence from a functional mouse model of breakdown and repair. Endocrinology 151:3386–3395.
27. Winterhager E, R Grummer, E Jahn, K Willecke and O Traub. (1993). Spatial and temporal expression of connexin26 and connexin43 in rat endometrium during trophoblast invasion. Dev Biol 157:399–409.
28. Kibschull M, A Gellhaus and E Winterhager. (2008). Analogous and unique functions of connexins in mouse and human placental development. Placenta 29:848–854.
29. Malassine A and L Cronier. (2005). Involvement of gap junctions in placental functions and development. Biochim Biophys Acta 1719:117–124.
30. Grummer R, SW Hewitt, O Traub, KS Korach and E Winterhager. (2004). Different regulatory pathways of endometrial connexin expression: preimplantation hormonal-mediated pathway versus embryo implantation-initiated pathway. Biol Reprod 71:273–281.
31. Fleming HE, V Janzen, C Lo Celso, J Guo, KM Leahy, HM Kronenberg and DT Scadden. (2008). Wnt signaling in the niche enforces hematopoietic stem cell quiescence and is necessary to preserve self-renewal in vivo. Cell Stem Cell 2:274–283.
32. Reya T, AW Duncan, L Ailles, J Domen, DC Scherer, K Willert, L Hintz, R Nusse and IL Weissman. (2003). A role for Wnt signalling in self-renewal of haematopoietic stem cells. Nature 423:409–414.
33. Habib SJ, BC Chen, FC Tsai, K Anastassiadis, T Meyer, E Betzig and R Nusse. (2013). A localized Wnt signal orients asymmetric stem cell division in vitro. Science 339:1445–1448.
34. Wang Y, M van der Zee, R Fodde and LJ Blok. (2010). Wnt/beta-catenin and sex hormone signaling in endometrial homeostasis and cancer. Oncotarget 1:674–684.
35. Ishikawa Y, H Ida-Yonemochi, H Suzuki, K Nakakura-Ohshima, HS Jung, MJ Honda, Y Ishii, N Watanabe and H Ohshima. (2010). Mapping of BrdU label-retaining dental pulp cells in growing teeth and their regenerative capacity after injuries. Histochem Cell Biol 134:227–241.
36. Brennand K, DW Huangfu and D Melton. (2007). All beta cells contribute equally to islet growth and maintenance. Plos Biol 5:1520–1529.
37. Patterson AL and JK Pru. (2013). Long-term label retaining cells localize to distinct regions within the female reproductive epithelium. Cell Cycle 12:2888–2898.
38. Taylor HS. (2004). Endometrial cells derived from donor stem cells in bone marrow transplant recipients. JAMA 292:81–85.
39. Gargett CE, KE Schwab, RM Zillwood, HP Nguyen and D Wu. (2009). Isolation and culture of epithelial progenitors and mesenchymal stem cells from human endometrium. Biol Reprod 80:1136–1145.
40. Meng X, TE Ichim, J Zhong, A Rogers, Z Yin, J Jackson, H Wang, W Ge, V Bogin, et al. (2007). Endometrial regenerative cells: a novel stem cell population. J Transl Med 5:57.
41. Welm BE, SB Tepera, T Venezia, TA Graubert, JM Rosen and MA Goodell. (2002). Sca-1(pos) cells in the mouse mammary gland represent an enriched progenitor cell population. Dev Biol 245:42–56.
42. Holmes C and WL Stanford. (2007). Concise review: stem cell antigen-1: expression, function, and enigma. Stem Cells 25:1339–1347.
43. Szotek PP, HL Chang, L Zhang, F Preffer, D Dombkowski, PK Donahoe and J Teixeira. (2007). Adult mouse myometrial label-retaining cells divide in response to gonadotropin stimulation. Stem Cells 25:1317–1325.
44. Wang Y, A Sacchetti, MR van Dijk, M van der Zee, PH van der Horst, R Joosten, CW Burger, JA Grootegoed, LJ Blok and R Fodde. (2012). Identification of quiescent, stem-like cells in the distal female reproductive tract. PLoS One 7:e40691.
45. Hu FF, X Jing, YG Cui, XQ Qian, YD Mao, LM Liao and JY Liu. (2010). Isolation and characterization of side population cells in the postpartum murine endometrium. Reprod Sci 17:629–642.
46. Tatsumi K, T Higuchi, H Fujiwara, T Nakayama, S Fujii and J Fujita. (2001). Expression of Ly-6A/E in the mouse uterus during implantation period. Mol Reprod Dev 58:159–165.
47. Schwab KE and CE Gargett. (2007). Co-expression of two perivascular cell markers isolates mesenchymal stem-like cells from human endometrium. Hum Reprod 22:2903–2911.
48. Fuchs E, T Tumbar and G Guasch. (2004). Socializing with the neighbors: stem cells and their niche. Cell 116:769–778.
49. Li L and T Xie. (2005). Stem cell niche: structure and function. Annu Rev Cell Dev Biol 21:605–631.
50. Tan J, S Raja, MK Davis, O Tawfik, SK Dey and SK Das. (2002). Evidence for coordinated interaction of cyclin D3 with p21 and cdk6 in directing the development of uterine stromal cell decidualization and polyploidy during implantation. Mech Dev 111:99–113.
51. Stewart CA, SJ Fisher, Y Wang, MD Stewart, SC Hewitt, KF Rodriguez, KS Korach and RR Behringer. (2011). Uterine gland formation in mice is a continuous process, requiring the ovary after puberty, but not after parturition. Biol Reprod 85:954–964.
52. Montfort I and R Perez-Tamayo. (1975). The distribution of collagenase in the rat uterus during postpartum involution. An immunohistochemical study. Connect Tissue Res 3:245–252.
53. Smith GH. (2005). Label-retaining epithelial cells in mouse mammary gland divide asymmetrically and retain their template DNA strands. Development 132:681–687.
54. Blanpain C, WE Lowry, A Geoghegan, L Polak and E Fuchs. (2004). Self-renewal, multipotency, and the existence of two cell populations within an epithelial stem cell niche. Cell 118:635–648.
55. Spradling A, D Drummond-Barbosa and T Kai. (2001). Stem cells find their niche. Nature 414:98–104.
56. Mills JC and JI Gordon. (2001). The intestinal stem cell niche: there grows the neighborhood. Proc Natl Acad Sci U S A 98:12334–12336.
57. Teng C, Y Guo, H Zhang, M Ding and H Deng. (2007). Identification and characterization of label-retaining cells in mouse pancreas. Differentiation 75:702–712.
58. Moore KA and IR Lemischka. (2006). Stem cells and their niches. Science 311:1880–1885.
59. Taylor G, MS Lehrer, PJ Jensen, TT Sun and RM Lavker. (2000). Involvement of follicular stem cells in forming not only the follicle but also the epidermis. Cell 102:451–461.

60. Wilson A, E Laurenti, G Oser, RC van der Wath, W Blanco-Bose, M Jaworski, S Offner, CF Dunant, L Eshkind, et al. (2008). Hematopoietic stem cells reversibly switch from dormancy to self-renewal during homeostasis and repair. Cell 135:1118–1129.
61. Lowry WE, C Blanpain, JA Nowak, G Guasch, L Lewis and E Fuchs. (2005). Defining the impact of beta-catenin/Tcf transactivation on epithelial stem cells. Genes Dev 19:1596–1611.
62. Zeng YA and R Nusse. (2010). Wnt proteins are self-renewal factors for mammary stem cells and promote their long-term expansion in culture. Cell Stem Cell 6:568–577.
63. Huang CC, GD Orvis, Y Wang and RR Behringer. (2012). Stromal-to-epithelial transition during postpartum endometrial regeneration. PloS One 7:e44285.
64. Patterson AL, L Zhang, NA Arango, J Teixeira and JK Pru. (2013). Mesenchymal-to-epithelial transition contributes to endometrial regeneration following natural and artificial decidualization. Stem Cells Dev 22:964–974.
65. Hugo H, ML Ackland, T Blick, MG Lawrence, JA Clements, ED Williams and EW Thompson. (2007). Epithelial—mesenchymal and mesenchymal—epithelial transitions in carcinoma progression. J Cell Physiol 213:374–383.
66. Morelli SS, P Rameshwar and LT Goldsmith. (2013). Experimental evidence for bone marrow as a source of nonhematopoietic endometrial stromal and epithelial compartment cells in a murine model. Biol Reprod 89:7.
67. Du H and HS Taylor. (2007). Contribution of bone marrow-derived stem cells to endometrium and endometriosis. Stem Cells 25:2082–2086.
68. Du H, H Naqvi and HS Taylor. (2012). Ischemia/reperfusion injury promotes and granulocyte-colony stimulating factor inhibits migration of bone marrow-derived stem cells to endometrium. Stem Cells Dev 21:3324–3331.

Address correspondence to:
Dr. Rachel W.S. Chan
Department of Obstetrics and Gynecology
LKS Faculty of Medicine
University of Hong Kong
Pokfulam
Hong Kong, SAR
China

E-mail: rwschan@hku.hk

Received for publication May 7, 2014
Accepted after revision November 10, 2014
Prepublished on Liebert Instant Online November 11, 2014